DOI: 10.1021/cg901181x

CRYSTAL GROWTH & DESIGN Article

2010, Vol. 10 806–811

Rational Assembly of d^{10} Metal−Organic Frameworks with Helical Nanochannels Based on Flexible V-Shaped Ligand

Hai-Long Jiang, Bo Liu, and Qiang Xu*

National Institute of Advanced Industrial Science and Technology (AIST), Ikeda, Osaka 563-8577, Japan

Received September 25, 2009; Revised Manuscript Received November 4, 2009

ABSTRACT: Solvothermal reactions of Zn(II) or Cd(II) nitrates and V-shaped ligand of 4,4′-(hexafluoroisopropylidene)bis(benzoic acid) (H_2hfipbb) in the presence or absence of 4,4′-bipy afforded four interesting d^{10} metal−organic frameworks with helical nanochannels, namely, Zn(hfipbb)·0.5H_2O·0.5DMF enantiomers ($P6_222$, **1a**, and $P6_422$, **1b**), Zn(hfipbb)(4,4′-bipy)·DMF (**2**), and Cd(hfipbb)(DMF)·0.5DMF (**3**). The enantiomeric **1a** and **1b** exhibit similarly a (4,4)-connected 3D network with two types of helically 2-fold and 8-fold nanochannels along the *c*-axis, in which ultralong helical pitches are found in the 8-fold helical channels. Compound **2** features a 2D layered structure based on dizinc(II) paddle-wheel clusters with the appearance of left- and right-hand helical channels alternatively, while 1D double helical channels exist in the complicated structure of compound **3**. The luminescent properties of all the compounds have also been studied.

Introduction

The design and synthesis of metal−organic frameworks (MOFs) are the focus of great interest in current research, not only because of their tremendous potential applications, such as gas storage and separation, heterogeneous catalysis, optical properties, etc., but also owing to their intriguing variety of architectures and topologies.[1−3] Compared with conventionally used microporous inorganic materials, such as zeolites, MOFs have advantages for more flexible and rational design by controlling the architecture and functionalizing the pores. The predesigned organic ligand is a vital component with binding sites in an appropriate arrangement, whose encoded information is read by the metal ions according to their coordination tendency.[4] On the other hand, helical structures are ubiquitous in nature and are the foundation of the genetic code, and they have attracted increased interest in coordination chemistry and material chemistry owing to their importance in biological systems, asymmetric catalysis, and optical devices.[5−7] A particular challenge in this field is design and synthesis of helical MOFs through the self-assembly of metal ions and ligands.[6] Although some helical layers and limited pillared-layer 3D MOFs with helical character have been reported,[7,8] the rational design and construction of helically structured MOFs are acutely hampered by limited understanding of the structural constraints in stabilizing the arrays.[9] Especially, it is particularly rare to obtain helically chiral MOFs by a route of spontaneous resolution without any chiral auxiliary.[10]

Inspired by the aforementioned considerations, our current synthetic strategy is to construct targeted MOFs with helical channels by employing a long and V-shaped aromatic dicarboxylate ligand, 4,4′-(hexafluoroisopropylidene)bis(benzoic acid) (H_2hfipbb). Herein, we successfully prepared four Zn and Cd compounds with helical channels, including a pair of enantiomers Zn(hfipbb)·0.5H_2O·0.5DMF ($P6_222$, **1a**, and $P6_422$, **1b**) with two types of 2-fold and 8-fold helical channels, Zn(hfipbb)(4,4′-bipy)·DMF (**2**) with left- and right-handed helical channels based on sharing the Zn(II) paddle-wheel clusters, and Cd(hfipbb)(DMF)·0.5DMF (**3**) with double helical channels. In these compounds, the structures change remarkably whereas the helical character is preserved during introduction of the second ligand of 4,4′-bipy or replacement of Zn(II) with Cd(II).

*E-mail: q.xu@aist.go.jp.

Experimental Section

Materials and General Methods. All the solvents and reagents for syntheses were commercially available and used as received. IR spectra were recorded on an attenuated total reflectance (ATR) FT-IR spectrometer (SensIR Technologies). Elemental analyses were performed on a Perkin-Elmer 2400 Series II analyzer. Thermogravimetric analyses (TGA) were carried out on a Shimadzu DTG-50 thermal analyzer from room temperature to 500 °C at a ramp rate of 5 °C/min in air. Powder X-ray diffraction (PXRD) studies were carried out with an X-ray diffractometer of Rigaku, Rint 2000. Solid state emission spectra were investigated on a Perkin-Elmer LS50B luminescence spectrophotometer under the same measurement conditions.

Syntheses of Compounds 1−3. Preparation of Zn(hfipbb)·0.5H_2O·0.5DMF (1a and 1b). A mixture of $Zn(NO_3)_2·4H_2O$ (0.106 g, 0.4 mmol), H_2hfipbb (0.157 g, 0.4 mmol), and DMF (10 mL) was sealed in a Teflon reactor. The pure colorless needle crystals containing **1a** and **1b** were obtained after 3 days of heating at 115 °C. Yield: 0.13 g, ∼70% (based on Zn). Anal. Calcd for $C_{18.5}F_6H_{12}N_{0.5}O_5Zn$: C, 44.30; H, 2.41; N, 1.40. Found: C, 44.92; H, 2.38; N, 1.50. IR (cm^{-1}): 1688 m, 1634 m, 1590 m, 1537 m, 1414 s, 1291 w, 1254 m, 1237 s, 1210 m, 1167 vs, 1152 m, 1136 m, 1090 w, 1022 w, 970 w, 959 w, 945 w, 928 m, 858 w, 847 w, 775 s, 748 m, 723 vs, 708 m, 685 w, 554 w, 544 w, 515 s, 488 m.

Preparation of Zn(hfipbb)(4,4′-bipy)·DMF (2). A mixture of Zn-$(NO_3)_2·4H_2O$ (0.106 g, 0.4 mmol), H_2hfipbb (0.157 g, 0.4 mmol), 4,4′-bipy (0.063 g, 0.4 mmol), and DMF (10 mL) was sealed in a Teflon reactor. The pure colorless needle crystals containing **2** were obtained after 3 days of heating at 115 °C. Yield: 0.09 g, ∼33% (based on Zn). Anal. Calcd for $C_{30}F_6H_{25}N_3O_5Zn$: C, 52.61; H, 3.69; N, 6.14. Found: C, 52.74; H, 3.47; N, 6.04. IR (cm^{-1}): 2520 b, 2012 b, 1676 m, 1645 s, 1615 w, 1408 vs, 1294 w, 1252 s, 1240 s, 1208 s, 1165 vs, 1136 m, 1088 w, 1071 w, 1046 w, 1020 w, 974 w, 959 m, 945 m, 930 m, 864 w, 845 m, 804 m, 781 vs, 747 m, 716 m, 687 w, 656 w, 625 s, 475 vs.

Preparation of Cd(hfipbb)(DMF)·0.5DMF (3). A mixture of $Cd(NO_3)_2·4H_2O$ (0.124 g, 0.4 mmol), H_2hfipbb (0.157 g, 0.4 mmol) with or without 4,4′-bipy (0.063 g, 0.4 mmol), and DMF (10 mL)

 Published on Web 12/01/2009

Table 1. Crystallographic Parameters for Compounds 1−3 from Single-Crystal X-ray Diffraction

complexes	1a	2b	2	3
formula	$C_{34}H_{16}F_{12}O_9Zn_2$	$C_{34}H_{16}F_{12}O_9Zn_2$	$C_{30}H_{24}F_6N_3O_5Zn$	$C_{20}H_{14}CdF_6NO_5$
FW	927.21	927.21	685.89	574.72
color	colorless	colorless	colorless	colorless
crystal system	hexagonal	hexagonal	monoclinic	orthorhombic
space group	$P6_222$	$P6_422$	$P2_1/c$	$Pccn$
a (Å)	21.250(3)	21.260(3)	13.080(3)	27.660(5)
b (Å)	21.250(3)	21.260(3)	9.7100(19)	7.4900(15)
c (Å)	7.7200(15)	7.7300(15)	25.530(8)	24.170(5)
α (deg)	90	90	90	90
β (deg)	90	90	105.26(3)	90
γ (deg)	120	120	90	90
V (Å^3)	3019.0(8)	3025.8(8)	3128.2(14)	5007.4(17)
Z	3	3	4	8
d_{calcd} (g/cm^3)	1.530	1.527	1.456	1.525
μ (mm^{-1})	1.295	1.292	0.863	0.944
T (K)	293(2)	293(2)	293(2)	293(2)
F(000)	1380	1380	1396	2264
Flack parameter	0.00(4)	0.01(4)		
reflns collected	28897	28486	29253	43185
independent reflns	2294 (R_{int} = 0.1082)	2307 (R_{int} = 0.0737)	7105 (R_{int} = 0.0391)	5708 (R_{int} = 0.0396)
obsd data [$I > 2\sigma(I)$]	1635	1773	5602	4140
data/restraints/parameters	2294/0/130	2307/0/132	7105/32/406	5708/0/299
GOF on F^2	0.988	1.052	1.020	1.100
$R1$, $wR2$ [$I > 2\sigma(I)$]	0.0608, 0.1485	0.0649, 0.1738	0.0462, 0.1371	0.0638, 0.1498
$R1$, $wR2$ (all data)	0.0859, 0.1646	0.0796, 0.1929	0.0610, 0.1516	0.0760, 0.1531

was sealed in a Teflon reactor. The pure colorless block crystals were obtained after 3 days of heating at 115 °C, followed by rinsing the as-obtained products with DMF, acetone, and ethanol. Yield: 0.15 g, ~58% (based on Cd). Anal. Calcd for $C_{21.5}F_6H_{18.5}CdN_{1.5}O_{5.5}$: C, 42.17; H, 3.05; N, 3.43. Found: C, 42.38; H, 2.98; N, 3.34. IR (cm^{-1}): 1680 w, 1649 m, 1597 m, 1551 m, 1391 vs, 1290 w, 1254 s, 1238 s, 1208 s, 1171 vs, 1136 m, 1109 m, 1020 w, 970 w, 959 w, 943 m, 928 m, 851 s, 779 vs, 747 m, 723 vs, 685 m, 521 w, 476 m, 451 s.

X-ray Crystallography. Single-crystal X-ray diffraction data for compounds **1**−**3** were collected on a R-AXIS RAPID II diffractometer at room temperature with Mo Kα radiation (λ = 0.71073 Å).[11] All the structures were solved by direct methods using the SHELXS program of the SHELXTL package and refined by full-matrix least-squares methods with SHELXL.[12] Metal atoms in each compound were located from the *E*-maps, and other non-hydrogen atoms were located in successive difference Fourier syntheses, where they were refined with anisotropic thermal parameters on F^2. Hydrogen atoms were located at geometrically calculated positions and refined with isotropic thermal parameters. For compounds **1** and **3**, isolated solvents within the channels were not crystallographically well-defined. The uncoordinated DMF molecules were determined on the basis of TGA and elemental microanalysis, and the data were treated with the SQUEEZE routine within PLATON.[13] Crystallographic data and structural refinements for compounds **1**−**3** are summarized in Table 1. Important bond lengths and angels are listed in Table 2. More details on the crystallographic studies as well as atom displacement parameters are given in the Supporting Information.

Table 2. Selected Bond Lengths (Å) and Bond Angles (deg) for Compounds 1−3[a]

1a			
Zn(1)−O(2)#1	1.912(5)	Zn(1)−O(2)#2	1.912(5)
Zn(1)−O(1)	1.934(5)	Zn(1)−O(1)#3	1.934(5)
1b			
Zn(1)−O(2)#1	1.927(5)	Zn(1)−O(2)#2	1.927(5)
Zn(1)−O(1)#3	1.945(5)	Zn(1)−O(1)	1.945(5)
2			
Zn(1)−O(1)	2.027(2)	Zn(1)−O(2)#1	2.035(2)
Zn(1)−N(2)	2.042(2)	Zn(1)−O(4)#2	2.042(2)
Zn(1)−O(3)#3	2.046(2)	Zn(1)−Zn(1)#1	2.9774(7)
O(1)−Zn(1)−O(2)#1	158.89(9)	O(1)−Zn(1)−N(2)	101.60(9)
O(2)#1−Zn(1)−N(2)	99.40(9)	O(1)−Zn(1)−O(4)#2	90.03(10)
O(2)#1−Zn(1)−O(4)#2	87.32(10)	N(2)−Zn(1)−O(4)#2	103.25(9)
O(1)−Zn(1)−O(3)#3	86.08(11)	O(2)#1−Zn(1)−O(3)#3	88.93(11)
N(2)−Zn(1)−O(3)#3	97.74(10)	O(4)#2−Zn(1)−O(3)#3	159.00(9)
3			
Cd(1)−O(1)#1	2.271(6)	Cd(1)−O(1)	2.271(6)
Cd(1)−O(3)#2	2.294(5)	Cd(1)−O(3)#3	2.294(5)
Cd(1)−O(4)#2	2.600(5)	Cd(1)−O(4)#3	2.600(5)
Cd(2)−O(5)#4	2.243(6)	Cd(2)−O(5)	2.243(6)
Cd(2)−O(2)#4	2.255(5)	Cd(2)−O(2)	2.255(5)
Cd(2)−O(4)#5	2.287(5)	Cd(2)−O(4)#2	2.287(5)

[a] Symmetry codes for **1a**: #1: $-y+1, -x+1, -z+{}^2/_3$; #2: $-y+1, x-y+1, z-{}^1/_3$; #3: $x, x-y+1, -z+{}^1/_3$. Symmetry codes for **1b**: #1: $-y+1, x-y, z+{}^1/_3$; #2: $x, x-y, -z-{}^1/_3$; #3: $-x+y+1, y, -z$. Symmetry codes for **2**: #1: $-x+1, -y, -z-1$; #2: $x, -y-{}^1/_2, z-{}^1/_2$; #3: $-x+1, y+{}^1/_2, -z-{}^1/_2$. Symmetry codes for **3**: #1: $-x+{}^1/_2, -y+{}^5/_2, z$; #2: $x, -y+{}^3/_2, z-{}^1/_2$; #3: $-x+{}^1/_2, y+1, z-{}^1/_2$; #4: $-x+{}^1/_2, -y+{}^3/_2, z$; #5: $-x+{}^1/_2, y, z-{}^1/_2$.

Results and Discussion

Zn(hfipbb)·0.5H$_2$O·0.5DMF (1a and 1b). Compounds **1a** and **1b** are enantiomers and exhibit similar structures. Therefore, **1a** will be discussed in detail as a representative. Compound **1a** crystallizes in chiral space group $P6_222$. It contains one crystallographically unique zinc(II) ion and an independent ligand in the asymmetric unit, both of which locate at the 2-fold axis with half-occupancies. Zn(1) is surrounded by a tetrahedral environment, in which the coordinated oxygen atoms come from four carboxylate anions of four hfipbb ligands. The Zn−O distances range from 1.912(5) to 1.935(5) Å, comparable to those reported for other zinc(II) compounds.[14] The hfipbb ligand is tetradentate, it bridges four zinc(II) ions, and each oxygen bonds with one Zn(II) (Scheme 1 and Figure S1 of the Supporting Information). The bent conformation of a dihedral angle between the two benzene rings in hfipbb ligand is 69.75°. The interconnection of zinc(II) ions by bridging hfipbb ligands results in a complicated 3D network with two types of helically hydrophilic and hydrophobic channels along the *c*-axis (Figures 1 and 2). The left-handed helically hydrophilic channel is quadrangular with channel dimensions of 6.47(1) Å × 6.47(1) Å (the shortest C···C distances based on structural data, Figures 2a and S3), of which the double helices have a helical pitch of 15.44 Å, equal to two times of *c*-axis length. The

Scheme 1. Coordination Modes of hfipbb Ligand in (a) 1 and 2, and in (b) 3

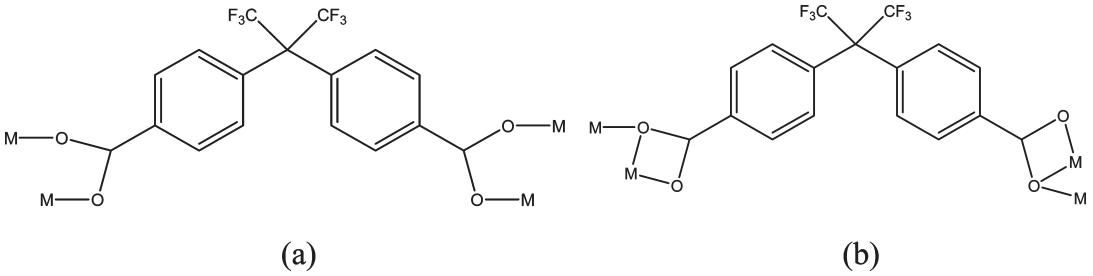

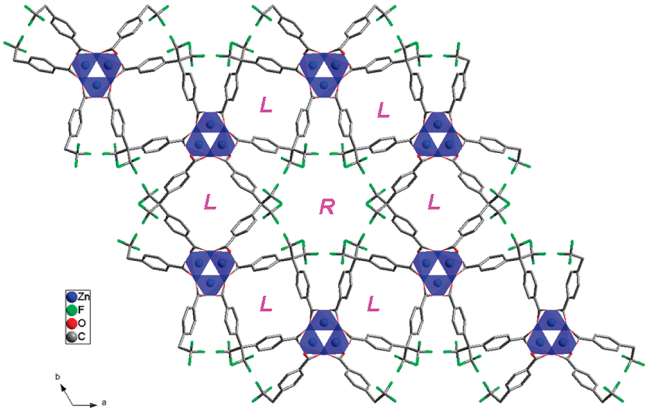

Figure 1. View of the 3D structure of **1a** along the *c*-axis. The hydrogen atoms and isolated water molecules are omitted for clarity. L and R indicate the left- and right-handed helical channels, respectively.

isolated aqua molecules are located in the quadrangular channels. The other right-handed helically hydrophobic channel along the *c*-axis with hexagonal shape has an absolutely free space of 7.990(6) × 7.990(6) Å^2 (shortest F···F distances based on structural data, Figures 2b and S3), which is composed by six Zn(1) atoms and six hfipbb ligands. The distance between diagonal Zn(1) atoms is 22.069(3) Å, and the fluorine atoms orient to the center of the channels. The right-handed helix is generated around the crystallographic 6_2 axis with a helical pitch of 61.75 Å, which is 8-fold the *c*-axis length. To the best of our knowledge, it is the most multiples of its corresponding axis length and close to the longest helical pitch (63.68 Å) presently known.[15] Notably, on the turning of the helix, the angle between the planes defined by two C−O−Zn−O−C chelate rings at one metal center is 104.44°, and the bent C7−C8−C7 angle in the hfipbb ligand is 112.17°, both of which lead to the helix coiling along the winding axis in a dodecagonal cross section (Figure S3). Most striking, however, is the fact that eight homochiral helical chains associate in parallel to form the wall of a dodecagonal nanochannel; its enantiomer can be found in **1b** (Figure 2). The chiral nanochannel assembled from 8-fold helices reported herein represents by far the second example of the highest degree of association of 1D motifs.[15]

A better insight into the nature of the involved framework can be achieved by the application of a topological approach. As described above, each Zn(II) ion is linked by four hfipbb ligands and each hfipbb ligand bridges four Zn(II) ions; therefore, both Zn(II) and hfipbb ligands can be regarded as four-connected nodes, and the whole network can be extended to an unusual 3D (4,4)-connected net with the Schläfli symbol of $(4^2\cdot8^2\cdot10^2)(4^2\cdot8^4)$,[16] as displayed in Figure 3. It should be noted that such a (4,4)-connected network observed in **1** is a new type, which is very different from other typical (4,4)-connected nets.[17]

So far, in the limited reports on chiral MOFs, most were synthesized by choosing chiral species (chiral organic linkers or chiral metal complexes) as structure directing agents.[18] While without any chiral auxiliary, to obain a chiral compound by using an achiral ligand under spontaneous resolution is possible but harder, because of the great difficulty to achieve interlinking of the chiral molecular units into a homochiral structure with high dimensionality and to induce spontaneous resolution. Compound Zn(hfipbb) with the $P6_422$ space group was reported recently by Monge et al., but they failed to obtain its enantiomer even when more than ten crystals were examined.[19] We successfully prepared the spontaneous resolution conglomerations in a one-pot reaction. Compounds **1a** and **1b** reveal the spontaneous resolution conglomeration in homochiral coordination polymers built from an achiral ligand. The effective free volume in **1** is 24.1% (total potential solvent volume of 726.5 Å^3 out of each unit cell volume of 3019.0 Å^3) calculated by PLATON.

Zn(hfipbb)(4,4′-bipy)·DMF (2). When introducing 4,4′-bipy into the Zn-hfipbb system, compound **2** was successfully obtained. The asymmetric unit of **2** consists of one zinc(II), one H_2hfipbb ligand, one 4,4′-bipy, and one DMF molecules. The basic second-building unit (SBU) of each dizinc(II) paddle-wheel cluster is coordinated by two 4,4′-bipy molecules and four carboxylic oxygens from four hfipbb^{2-} anions. Such tetracarboxylate-bridged dimetallic (e.g., Cu_2^{4+} and Zn_2^{4+}) paddle wheels have been investigated as SBUs for the construction of porous MOFs that display gas storage and separation properties.[20] In the dizinc(II) unit, the bond distances between Zn and carboxylic oxygens are in the range of 2.027(2)−2.046(2) Å, which is similar to a Zn−N distance of 2.042(2) Å. The intradimer Zn−Zn separation is 2.9774(7) Å, all of which are comparative to those reported.[20c,d] The coordination mode of the hfipbb ligand is similar to that in **1a** (Scheme 1), and the bent conformation gives a dihedral angle of 75.59° between the two benzene rings, slightly bigger than that in **1a**. Notably, each dinuclear Zn(II) paddle-wheel cluster connects with the other four neighboring ones by the bent hfipbb ligands, leading to an undulating (4, 4) net with a rhombic window (Figure 4a). The window sizes between adjacent centers of dinuclear zinc subunits of the net are 13.639(4) × 13.639(4) Å^2. As shown in Figure 4, the left- and right-hand helical chains appear alternatively by sharing the paddle-wheel clusters, resulting in the formation of the 1D helical nanochannels in the covalent skeleton of this 2D sheet, with two DMF molecules located in each channel. The effective free volume in **2** is 27.1% (total potential solvent volume of 848.0 Å^3 out of each unit cell volume of 3128.2 Å^3) by the PLATON calculation.

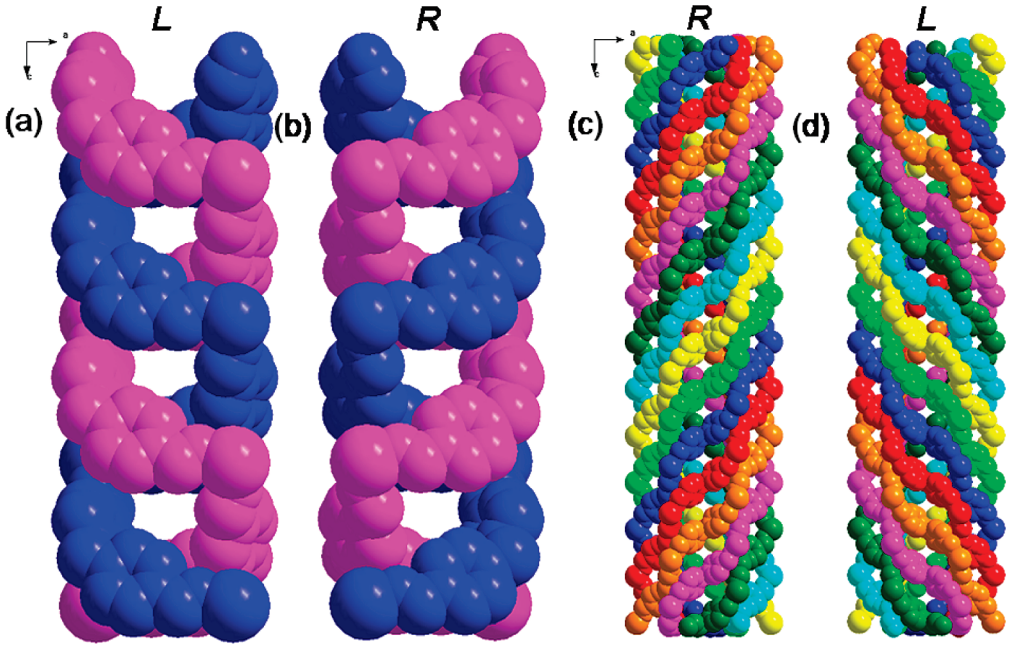

Figure 2. Space-filling representation of enantiomeric double helices in (a) **1a** and (b) **1b**, and octuple helices in (c) **1a** and (d) **1b**, highlighting the extra long pitch. L and R indicate the left- and right-handed helical chains, respectively.

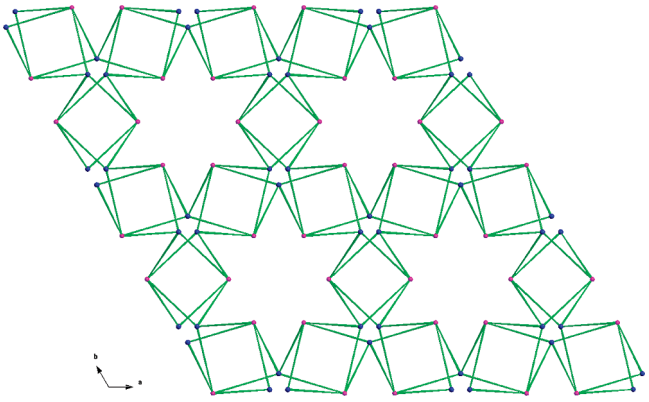

Figure 3. Topological view of the 3D network of **1a** along the *c*-axis.

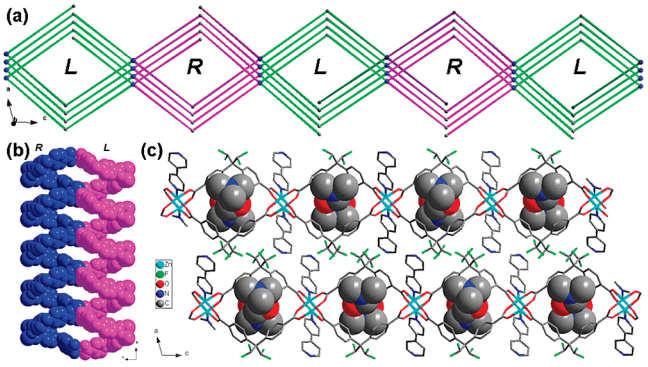

Figure 4. (a) Schematic representation of 1D helical channels in 2D layers in **2**. (b) Space-filling representation of the left- and right-handed chains. (c) View of the structure of **2** along the *b*-axis; DMF molecules located in the helical channels are highlighted by space-filling mode.

Cd(hfipbb)(DMF)·0.5DMF (3). Compound **3** was obtained when we tried to replace Zn with Cd, but the 4,4′-bipy molecule was not coordinated in the Cd system even if it was added as a reagent. There are two crystallographically independent Cd(II) centers in the asymmetric unit. Compared with Zn(II), Cd(II) usually adopts more coordinated atoms, owing to a larger ion radius. The Cd(1) atom is coordinated by six oxygens with a seriously distorted octahedral configuration. There are also two weak Cd−O contacts of 2.671(0) Å, which can be considered as secondary coordination bonds. All eight oxygens are from four separate hfipbb ligands in a chelated bidentate coordination fashion. The Cd(2) atom in the lattice presents a classical six-coordinate octahedral configuration with two symmetric DMF molecules on the axial vertex and four separate monondentate carboxylate oxygen atoms on the basal plane. All the Cd−O and Cd−N bond distances fall into the normal ranges.[15] The unique H_2hfipbb ligand in the bent conformation gives a dihedral angle of 72.94° between the two benzene rings, which bridges two Cd(2) atoms and chelates bidentately two Cd(1) atoms (Scheme 1, Figure S5). In such a connection, each Cd(1) connects with the other four neighboring ones by sharing the bent hfipbb ligands, leading to an undulating (4,4) net with a rhombic window (Figure 5a). The window sizes between adjacent centers of Cd(1) of the net are 14.218(2) × 14.218(2) $Å^2$, which is similar to that in **2**. But the existing difference in them is the two identical helical layers are interpenetrated to present parallel 2D to 2D layers in **3** (Figure 5a and b). Upon 2-fold parallel interpenetration, the 1D double helical nanochannels are formed. The Cd(2) ions are connected by hfipbb ligands and DMF molecules to form a linear chain along the *c*-axis (Figure 5c). Such chains are further interconnected with the helical double-layers by sharing hfipbb ligands into a complicated layered structure of compound **3** (Figure S6).

Thermal Stability Analyses. To examine the thermal stability of compounds **1**−**3**, thermal gravimetric (TG) analyses were carried out (Figure S8). The TG curve of **1** exhibits two steps of weight loss. The first weight loss is 9.00% in the temperature range of 85−230 °C, which corresponds to the

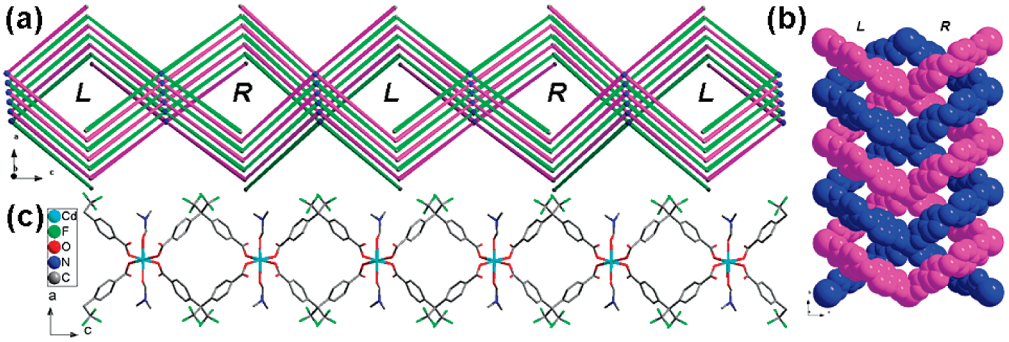

Figure 5. (a) Schematic representation of 1D double helical channels formed by interconnection of Cd(1) and hfipbb ligands in **3**. (b) Space-filling representation of double-stranded helical structures. (c) View of the linear chain of Cd(2) with hfipbb ligands and DMF molecules.

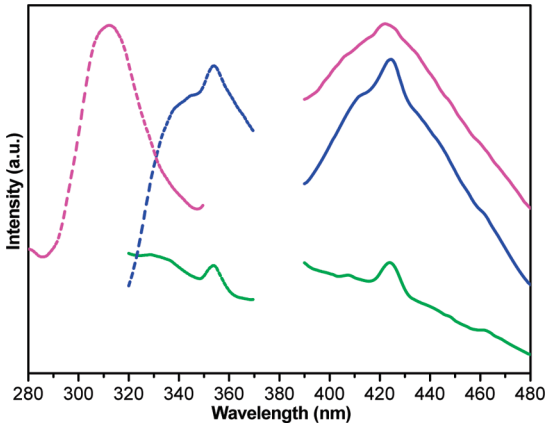

Figure 6. Solid-state emission spectra (right) of compounds at room temperature: **1** (green), **2** (blue), and **3** (cyan). The corresponding excitation bands are marked as dotted lines on the left.

loss of isolated water and DMF molecules (calcd 9.09%), followed by a plateau. The framework starts to decompose at around 300 °C and does not end until 500 °C. Compound **2** starts to lose uncoordinated DMF molecules around 100 °C, followed by decomposition of the organic ligands. It gives a total weight loss of 88.26% in the range of 100−490 °C, which agrees with the calculated value of 88.12%. The remaining weight of 11.74% indicated that the final product was ZnO (calcd 11.88%). In contrast, three steps of weight losses happen to compound **3**. The weight loss between 60 and 200 °C corresponds to the release of isolated DMF molecules (calcd 5.95%, obsd 5.67%), immediately followed by losing the coordinated DMF until around 280 °C (calcd 11.90%, obsd 11.50%). The framework stabilizes until around 340 °C, and the organic ligand starts to combust upon further heating.

Photoluminescence Properties. Taking into account the excellent luminescent properties of d^{10} metal complexes, the solid-state luminescence of compounds **1**−**3** was investigated. It can be observed that strong emissions occur at around 425 nm for **2** and **3**, under λ_{ex} = 354 nm (for **2**) and 313 nm (for **3**), whereas weaker fluorescence occurs at the same position for **1** under λ_{ex} = 354 nm (Figure 6). To understand the nature of the emission band, the photoluminescence properties of the H_2hfipbb ligand were also analyzed. It was found that the weak emission at 595 nm could be observed for free H_2hfipbb ligand under λ_{ex} = 435 nm (Figure S9). The lower intensities of the emission bands for compound **1** compared with **2** and **3** are possibly due to the quenching effect of the luminescent state by high-frequency vibrating water molecules.[21] The emission bands for **1**−**3** may be due to σ-donation from the carboxylate ligands to the Zn(II) or Cd(II) center and are tentatively attributed to the ligand-to-metal charge transfer (LMCT).[22] The photoluminescence properties of these compounds indicate that compounds **2** and **3** may be candidates for potential photoactive materials.

Conclusion

In summary, we have developed a rational synthetic strategy that successfully provides four helical d^{10} metal−hfipbb complexes by properly choosing the V-shaped dicarboxylate ligand. Even though the H_2hfipbb ligand displays different coordination modes and the DMF molecules play various roles in different compounds—bonding with a metal center or remaining uncoordinated inside the helical channels, the helical character always exists in these compounds. The successful isolation of four solid materials not only affords new complexes with interesting structures but also helps us to further understand the essence of helix character. The rational design idea depicted in this work may be a promising technique for the exploration of many other novel MOFs with helical or chiral characters.

Acknowledgment. The authors are thankful to AIST and JSPS for financial support. H.-L.J. thanks the JSPS for postdoctoral fellowship.

Supporting Information Available: X-ray crystallographic files for compounds **1**−**3** in CIF format; and XRD powder patterns, TG curves, emission spectra of H_2hfipbb ligand, molecular parameters, structures, and ORTEP drawings in PDF format. This material is available free of charge via the Internet at http://pubs.acs.org.

References

(1) (a) Pan, L.; Parker, B.; Huang, X. Y.; Olson, D. H.; Lee, J. Y.; Li, J. *J. Am. Chem. Soc.* **2006**, *128*, 4180. (b) Britt, D.; Tranchemontagne, D.; Yaghi, O. M. *Proc. Natl. Acad. Sci. U.S.A.* **2008**, *105*, 11623. (c) Férey, G.; Mellot-Draznieks, C.; Serre, C.; Millange, F.; Dutour, J.; Surblé, S.; Margiolaki, I. *Science* **2005**, *309*, 2040. (d) Kitaura, R.; Seki, K.; Akiyama, G.; Kitagawa, S. *Angew. Chem., Int. Ed.* **2003**, *42*, 428. (e) Wu, C. D.; Lin, W. *Angew. Chem., Int. Ed.* **2007**, *46*, 1075. (f) Zou, R. Q.; Sakurai, H.; Han, S.; Zhong, R. Q.; Xu, Q. *J. Am. Chem. Soc.* **2007**, *129*, 8402. (g) Liu, B.; Shioyama, H.; Akita, T.; Xu, Q. *J. Am. Chem. Soc.* **2008**, *130*, 5390. (h) Jiang, H. L.; Liu, B.; Akita, T.; Haruta, M.; Sakurai, H.; Xu, Q. *J. Am. Chem. Soc.* **2009**, *131*, 11302.

(2) (a) Ouellette, W.; Prosvirin, A. V.; Whitenack, K.; Dunbar, K. R.; Zubieta, J. *Angew. Chem., Int. Ed.* **2009**, *48*, 2140. (b) Zhang, Y.-B.; Zhang, W.-X.; Feng, F.-Y.; Zhang, J.-P.; Chen, X.-M. *Angew. Chem., Int. Ed.* **2009**, *48*, 5287. (c) Chen, B.; Yang, Y.; Zapata, F.; Lin, G.; Qian, G.; Lobkovsky, E. B. *Adv. Mater.* **2007**, *19*, 1693. (d) Song, J. L.; Mao, J. G. *Chem.—Eur. J.* **2005**, *11*, 1417.

(3) (a) Batten, S. R.; Robson, R. *Angew. Chem., Int. Ed.* **1998**, *37*, 1460. (b) Du, M.; Jiang, X. J.; Zhao, X. J. *Chem. Commun.* **2005**, 5521. (c) Wang, X. L.; Qin, C.; Wang, E. B.; Li, Y. G.; Su, Z. M.; Xu, L.; Carlucci, L. *Angew. Chem., Int. Ed.* **2005**, *44*, 5824.
(4) Lehn, J.-M. *Supramolecular Chemistry: Concepts and Perspectives*; VCH: Weinheim, Germany, 1995.
(5) (a) Moulton, B.; Zaworotko, M. J. *Chem. Rev.* **2001**, *101*, 1629. (b) Soghomonian, V.; Chen, Q.; Haushalter, R. C.; Zubieta, J.; O'Connor, C. J. *Science* **1993**, *259*, 1596. (c) Shi, Z.; Feng, S. H.; Gao, S.; Zhang, L.; Yang, G.; Hua, J. *Angew. Chem., Int. Ed.* **2000**, *39*, 2325. (d) Gier, T. E.; Bu, X.; Feng, P.; Stucky, G. D. *Nature* **1998**, *395*, 154. (e) Neeraj, S.; Natarajan, S.; Rao, C. N. R. *Chem. Commun.* **1999**, 165. (f) Kumaran, D.; Eswaramoorthy, S.; Studier, F. W.; Swaminathan, S. *Protein Sci.* **2005**, *14*, 719.
(6) (a) Cui, Y.; Lee, S. J.; Lin, W. *J. Am. Chem. Soc.* **2003**, *125*, 6014. (b) Zhang, J.-P.; Lin, Y.-Y.; Huang, X.-C.; Chen, X.-M. *Chem. Commun.* **2005**, 1258. (c) Wang, X. L.; Qin, C.; Wang, E. B.; Xu, L.; Su, Z. M.; Hu, C. W. *Angew. Chem., Int. Ed.* **2004**, *43*, 5036. (d) Sun, D. F.; Cao, R.; Sun, Y. Q.; Bi, W. H.; Li, X.; Hong, M. C.; Zhao, Y. J. *Eur. J. Inorg. Chem.* **2003**, 38.
(7) (a) Han, L.; Hong, M. C.; Wang, R. H.; Luo, J. H.; Lin, Z. Z.; Yuan, D. Q. *Chem. Commun.* **2003**, 2580. (b) Liang, J.; Wang, Y.; Yu, J. H.; Li, Y.; Xu, R. R. *Chem. Commun.* **2003**, 882.
(8) (a) Xiao, D.-R.; Wang, E.-B.; An, H.-Y.; Li, Y.-G.; Su, Z.-M.; Sun, C.-Y. *Chem.—Eur. J.* **2006**, *12*, 6528. (b) Han, L.; Zhou, Y.; Zhao, W. N.; Li, X.; Liang, Y. X. *Cryst. Growth Des.* **2009**, *9*, 660.
(9) (a) Langford, S. J.; Woodward, C. P. *CrystEngComm* **2007**, *9*, 218. (b) Du, M.; Zhang, Z. H.; Guo, W.; Fu, X. J. *Cryst. Growth Des.* **2009**, *9*, 1655.
(10) (a) Rao, A. S.; Pal, A.; Ghosh, R.; Das, S. K. *Inorg. Chem.* **2009**, *48*, 1802. (b) Ou, G.-C.; Jiang, L.; Feng, X.-L.; Lu, T.-B. *Inorg. Chem.* **2008**, *47*, 2710.
(11) Higashi, T. *Program for Absorption Correction*; Rigaku Corporation: Tokyo, Japan, 1995.
(12) Sheldrick, G. M. *SHELXTL NT, Program for Solution and Refinement of Crystal Structures*, version 5.1; University of Göttingen: Göttingen, Germany, 1997.
(13) Spek, A. L. *Acta Crystallogr., Sect. A* **1990**, *46*, C34.
(14) (a) Liu, G. X.; Huang, Y. Q.; Chu, Q.; Okamura, T.; Sun, W. Y.; Liang, H.; Ueyama, N. *Cryst. Growth Des.* **2008**, *8*, 3233. (b) Yang, Q. Z.; Siri, O.; Braunstein, P. *Chem. Commun.* **2005**, 2660. (c) Sun, Z. M.; Mao, J. G.; Sun, Y. Q.; Zeng, H. Y.; Clearfield, A. *Inorg. Chem.* **2004**, *43*, 336.
(15) Hao, X. R.; Wang, X. L.; Qin, C.; Su, Z. M.; Wang, E. B.; Lan, Y. Q.; Shao, K. Z. *Chem. Commun.* **2007**, 4620.
(16) (a) Wells, A. F. *Three-Dimensional Nets and Polyhedra*; Wiley: New York, 1977. (b) Robson, R. *J. Chem. Soc., Dalton Trans.* **2000**, 3735–3744.
(17) (a) Zhong, R. Q.; Zou, R. Q.; Du, M.; Yamada, T.; Maruta, G.; Takeda, S.; Xu, Q. *Dalton Trans.* **2008**, 2346. (b) Wang, S.; Bai, J.; Xing, H.; Li, Y.; Song, Y.; Pan, Y.; Scheer, M.; You, X. *Cryst. Growth Des.* **2007**, *7*, 747. (c) Guo, X. D.; Zhu, G. S.; Li, Z. Y.; Chen, Y.; Li, X. T.; Qiu, S. L. *Inorg. Chem.* **2006**, *45*, 4065.
(18) (a) Seo, J. S.; Whang, D.; Lee, H.; Jun, S. I.; Oh, J.; Jeon, Y. J.; Kim, K. *Nature* **2000**, *404*, 982. (b) Wu, C. D.; Hu, A.; Zhang, L.; Lin, W. *J. Am. Chem. Soc.* **2005**, *127*, 8940. (c) Zhang, J.; Chen, S.; Valle, H.; Wong, A. M. C.; Cruz, M.; Bu, X.-H. *J. Am. Chem. Soc.* **2007**, *129*, 14168.
(19) Monge, A.; Snejko, N.; Gutiérrez-Puebla, E.; Medina, M.; Cascales, C.; Ruiz-Valero, C.; Iglesias, M.; Gómez-Lor, B. *Chem. Commun.* **2005**, 1291.
(20) (a) Pan, L.; Olson, D. H.; Ciemnolonski, L. R.; Heddy, R.; Li, J. *Angew. Chem., Int. Ed.* **2006**, *45*, 616. (b) Chui, S. S.-Y.; Lo, S. M.-F.; Charamant, J. P. H.; Orpen, A. G.; Williams, I. D. *Science* **1999**, *283*, 1148. (c) Chun, H.; Dybtsev, D. N.; Kim, H.; Kim, K. *Chem.—Eur. J.* **2005**, *11*, 3521. (d) Moulton, B.; Abourahma, H.; Bradner, M. W.; Lu, J. J.; McManus, G. J.; Zaworotko, M. J. *Chem. Commun.* **2003**, 1342.
(21) Song, J.-L.; Lei, C.; Mao, J.-G. *Inorg. Chem.* **2004**, *43*, 5630.
(22) (a) Luo, J. H.; Hong, M. C.; Wang, R. H.; Cao, R.; Han, L.; Lin, Z. Z. *Eur. J. Inorg. Chem.* **2003**, 2705. (b) Wang, X. L.; Qin, C.; Wang, E. B.; Su, Z. M. *Chem.—Eur. J.* **2006**, *12*, 2680. (c) Jiang, H. L.; Huang, S. P.; Fan, Y.; Mao, J. G.; Cheng, W. D. *Chem.—Eur. J.* **2008**, *14*, 1972.